TRANSPORT PROBLEMS 2023 Volume 18 Issue 2
PROBLEMY TRANSPORTU DOI:10.20858/tp.2023.18.2.18

Keywords: vehicle dynamics model; dynamic optimization; lane change and overtaking maneuvers

Michał BRZOZOWSKI[1], Łukasz DRĄG[2*]

APPLICATION OF DYNAMIC OPTIMIZATION FOR AUTONOMOUS VEHICLE MOTION CONTROL

Summary. This article presents a procedure algorithm and vehicle dynamics models that can be applied to planning and controlling the motion of an autonomous car. The simulation results obtained using a simplified bicycle model with three degrees of freedom and a spatial model with 10 degrees of freedom were compared. The numerical efficiency of both models was evaluated. The task of dynamic optimization was formulated, the solution to which enables the implementation of lane change and overtaking maneuvers. The task was solved using the bicycle model, and the results (implementation of the intended maneuver) were validated using the spatial model.

1. INTRODUCTION

Autonomous vehicle-related technologies have been rapidly developing in recent years. This is a leading topic widely studied in many research and academic centers engaged in vehicle and transport research. Although no fully autonomous commercial vehicle has yet appeared, autonomous driving systems and other technologies derived from autonomous vehicle designs and prototypes are widely used in many vehicles currently on the market – for example, in the form of lane-keeping assistance or active cruise control.

Autonomous vehicles aggregate inventions and technologies from different fields of science, combining them into a common complementary system that must be precise and reliable yet effective in their operation so that the autonomous vehicle can respond in real time to changing road conditions. Similarly, the autonomous vehicle motion model differs from the classic vehicle motion model. It must be numerically efficient, reliable, as accurate (precise) as possible, and easy to implement. The autonomous vehicle motion model should be able to predict (plan) vehicle motion based on signals received from measuring devices while maintaining performance and speed. Finding a compromise between these requirements is not easy.

Issues related to the modeling of vehicle kinematics and dynamics have a very extensive literature. Many technical universities and research centers related to automotive technology are engaged in this endeavor [9]. In general, two main trends in modeling can be distinguished. Researchers of the first trend try to develop models that, as much as possible, reflect a vehicle's features and properties. It produces models with many degrees of freedom, nonlinear, requiring high computing power in motion (dynamics) simulations [1, 11]. If professional vehicle dynamics simulation packages such as MSC, ADAMS, and DADS are used for testing, the cost of such tests increases significantly.

The other trend includes models as simplified as possible with low computing power requirements but which reflect the main characteristics of moving vehicles. Their main advantage is their numerical efficiency, with which they can be used for the real-time control of vehicles or in dynamic optimization. Examples of such models can be found, inter alia, in the literature [8, 10]. The first was used to simulate

[1] University of Bielsko-Biala, Faculty of Mechanical Engineering and Computer Science; Willowa 2, 43-309 Bielsko-Biala, Poland; email: mbrzozowski@ath.bielsko.pl; orcid.org/0000-0001-9272-6594
[2] University of Bielsko-Biala, Faculty Management and Transport; Willowa 2, 43-309 Bielsko-Biala, Poland; email: ldrag@ath.bielsko.pl; orcid.org/0000-0001-7947-1726
*Corresponding author. E-mail: ldrag@ath.bielsko.pl

the motion and collisions of multi-member vehicles, while the second model was used to analyze the effect of the castor offset on the braking stability of a vehicle with ABS (Anti-lock Braking System) a surface of the μ- split type.

This paper presents two models of passenger vehicles. The first is the spatial model (SM), formulated using modeling methods adopted in robotics and having 10 degrees of freedom [3. 4]. In this model, three translational coordinates (body center of mass positions) and the rotational coordinates (ZYX Euler angles) were used to describe the position of the vehicle as a rigid body. The other four degrees of freedom of the system are due to the wheel steering angle of the vehicle. Homogeneous transformations were used to describe the geometry and coordinate transformations.

The other model is a flat bicycle model (BM) with three degrees of freedom only. It is widely used for autonomous vehicle control [2, 5, 6, 12].

As part of this study, the vehicle dynamics models were validated, their numerical efficiency was evaluated, and then the task of dynamic optimization was formulated. Its solution, consisting of the determination of the steering angle of the vehicle's front wheels, ensures the implementation of the intended maneuver (lane change or overtaking). The final part of this paper presents the options for applying optimization methods to autonomous vehicle motion control using the models presented in this paper.

2. SPATIAL INTRODUCTION

The method of homogeneous transformations was used to formulate this model, patterned after the spatial models from the literature [4]. The motion of a vehicle body, as shown in Fig. 1 (i.e., the body with suspensions), is described by the following components of the vector:

$$\mathbf{q}_b = \begin{bmatrix} \mathbf{r}_c \\ \boldsymbol{\phi} \end{bmatrix}, \tag{1}$$

where: $\mathbf{r}_c = \begin{bmatrix} x_c \\ y_c \\ z_c \end{bmatrix}$ – vector specifying the position of the vehicle's center of mass,

$\boldsymbol{\phi} = \begin{bmatrix} \psi \\ \theta \\ \varphi \end{bmatrix}$ – vector specifying the orientation of the axis of the coordinate system associated with the vehicle $\{\}'$ relative to the axis of the inertial system $\{\}$,

ψ, θ, φ – Euler's ZYX angles.

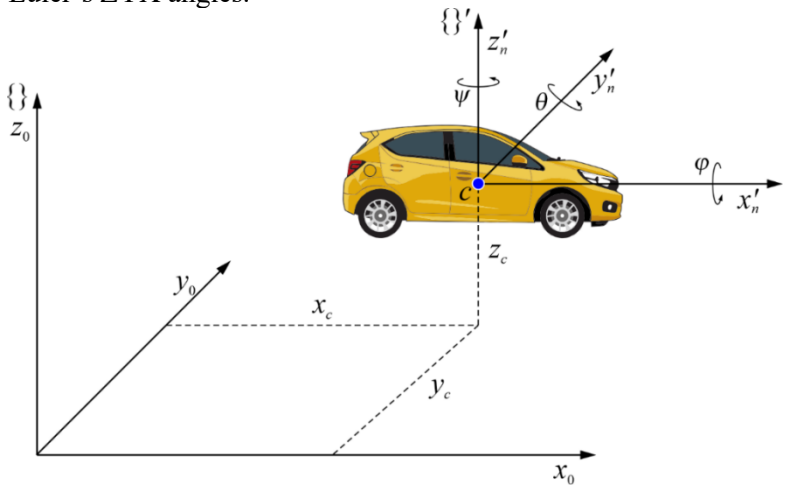

Fig. 1. Position of a vehicle in an inertial system $\{\}$ – *Spatial Model* (SM). Generalized coordinates of the vehicle body

Coordinates are transformed from system $\{\}'$ to system $\{\}$ according to dependence:

$$\mathbf{r} = \mathbf{B}\,\mathbf{r}'_b, \tag{2}$$

where: $\mathbf{r} = \begin{bmatrix} x \\ y \\ z \\ 1 \end{bmatrix}$ – vector of coordinates of a point in the system {},

$\mathbf{r'}_b = \begin{bmatrix} x' \\ y' \\ z' \\ 1 \end{bmatrix}$ – vector of coordinates of a point in the system {}′,

$\mathbf{B} = \mathbf{B}(\mathbf{q}_\mathrm{b}) = \begin{bmatrix} \mathbf{R} & \mathbf{r}_c \\ \mathbf{0} & 1 \end{bmatrix}$ – transformation matrix,

$$\mathbf{R} = \begin{bmatrix} \cos\psi & -\sin\psi & 0 \\ \sin\psi & \cos\psi & 0 \\ 0 & 0 & 1 \end{bmatrix} \begin{bmatrix} \cos\theta & 0 & \sin\theta \\ 0 & 1 & 0 \\ -\sin\theta & 0 & \cos\theta \end{bmatrix} \begin{bmatrix} 1 & 0 & 0 \\ 0 & \cos\varphi & -\sin\varphi \\ 0 & \sin\varphi & \cos\varphi \end{bmatrix}.$$

It was assumed that the suspension susceptibility can be reduced to the vehicle's tires. Therefore, the movement of the wheels relative to the body is described by φ_i (the angle of wheel rotation) and δ_i (the angle of wheel steering), $i = 1, 2, 3, 4$ (Fig. 2).

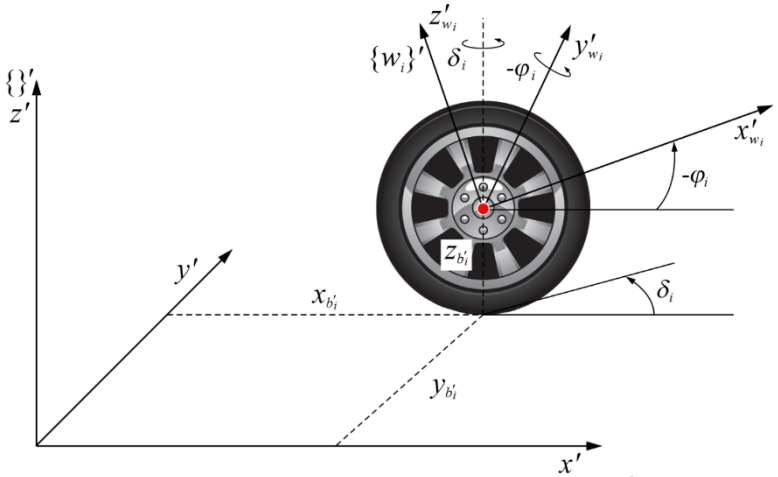

Fig. 2. Angles: φ_i – angle of wheel rotation and δ_i – angle of the i^{th} wheel steering

Coordinates with the wheel system i $\{w_i\}'$ to the system {}′ associated with the vehicle b, were transformed according to the dependence:

$$\mathbf{r}'_\mathrm{i} = \mathbf{D}_i \mathbf{W}_i \mathbf{r'}_{w,i} \tag{3}$$

where: $\mathbf{D}_i = \begin{bmatrix} \mathbf{\Omega}_i & \mathbf{r'}_{b,i} \\ \mathbf{0} & 1 \end{bmatrix}$, $\mathbf{\Omega}_i = \begin{bmatrix} \cos\delta_i & -\sin\delta_i & 0 \\ \sin\delta_i & \cos\delta_i & 0 \\ 0 & 0 & 1 \end{bmatrix}$,

$\mathbf{W}_i = \begin{bmatrix} \mathbf{\Lambda}_i & 0 \\ \mathbf{0} & 1 \end{bmatrix}$, $\mathbf{\Lambda}_i = \begin{bmatrix} \cos\varphi_i & 0 & \sin\varphi_i \\ 0 & 1 & 0 \\ -\sin\varphi_i & 0 & \cos\varphi_i \end{bmatrix}$.

Moreover, coordinates were transformed from the wheel system $\{w_i\}'$ to the inertial system {} by dependency:

$$\mathbf{r} = \mathbf{B}\,\mathbf{D}_i \mathbf{W}_i\, \mathbf{r'}_{w,i}. \tag{4}$$

It was assumed in this study that the angles of δ_i are known functions of time:

$\begin{cases} \delta_1 = \delta_2 = \delta(t) & \text{– front wheel steering angle} \\ \delta_3 = \delta_4 = 0 & \text{– rear wheel steering angle.} \end{cases}$

Thus, the number of degrees of freedom of the vehicle with wheels was reduced to 10:

$$\mathbf{q} = \begin{bmatrix} \mathbf{q}_b \\ \mathbf{q}_\varphi \end{bmatrix}, \tag{5}$$

where: $\mathbf{q}_b$ is defined in (1),

$$\mathbf{q}_\varphi = \begin{bmatrix} \varphi_1 \\ \varphi_2 \\ \varphi_3 \\ \varphi_4 \end{bmatrix}, \tag{6}$$

where: φ_i – wheel rotation angle i.

The interaction between the wheels and the roadway was described according to the Dugoff-Uffelman model [4]. The vehicle motion equations were written in the form

$$\mathbf{M}(\mathbf{q})\ddot{\mathbf{q}} = \boldsymbol{f}\left(\mathbf{q}, \dot{\mathbf{q}}, \delta(t)\right) \tag{7}$$

and were integrated by the Runge-Kutta method of the fourth order with a constant integration step. Initial conditions for dynamics were determined by solving a system of nonlinear algebraic equations describing the static equilibrium of the vehicle.

3. SIMPLIFIED MODEL (BICYCLE MODEL)

The BM is a flat model with three degrees of freedom (3 DoF) and is shown in Fig. 3.

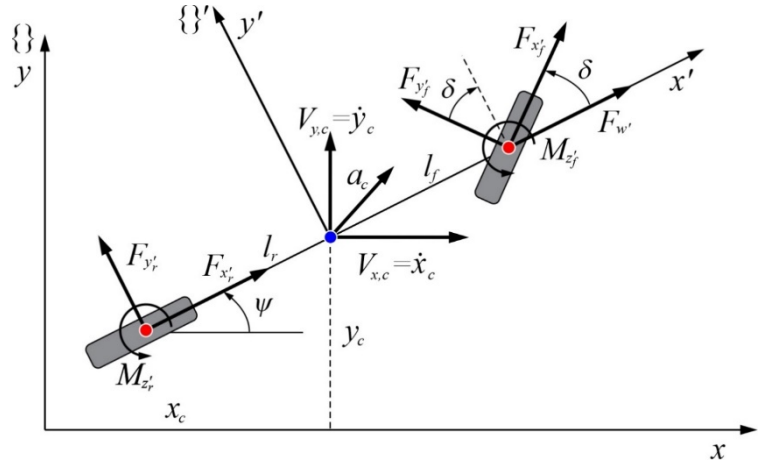

Fig. 3. Vehicle diagram – simplified model (BM)

Vehicle motion equations in the x, y coordinate system can be written as follows:

$$m\,\ddot{x}_c = F_{x',r}\cos\psi - F_{y',r}\sin\psi + F_{x',r}\cos(\delta+\psi) - F_{y',f}\sin(\delta+\psi) - F_{w'}\cos\psi, \tag{8}$$

$$m\,\ddot{y}_c = F_{x',r}\sin\psi + F_{y',r}\cos\psi + F_{x',f}\sin(\delta+\psi) + F_{y',f}\cos(\delta+\psi) - F_{w'}\sin\psi, \tag{9}$$

$$I_z\ddot{\psi} = -F_{y',r}l_r + F_{x',f}l_f\sin\delta + F_{y',f}l_f\cos\delta + M_{z',r} + M_{z',f}, \tag{10}$$

where: m – total mass of the vehicle (with wheels),

$I_{z'}$ – mass moment of inertia of the vehicle relative to the axle z' perpendicular to the plane x, y and placed in the center of mass C,

x_c, y_c– vehicle mass center coordinates,

δ – steering angle of the front wheels,

ψ – angle of inclination of the vehicle's longitudinal axis the x inertial system {} axis,

$F_{x',r}$, $F_{y',r}$ – component forces in the plane x', y' acting on the rear wheels of the vehicle,

$F_{x',f}$, $F_{y',f}$ – component forces in the plane x', y' acting on the front wheels of the vehicle,

l_r, l_f – distance of the vehicle's rear and front axles from its mass center,

$F_{w'}$ – air resistance force,

$M_{z',r}, M_{z',f}$ – stabilizing moments.

Three ways to determine the forces of roadway impacts on vehicles were considered. Table 1 summarizes the means of determining forces and moments, assuming that the vehicle is moving at V_{nom}, which is the longitudinal velocity of the vehicle, adopted as a known function of time. Slip angles α_r *i* α_f were determined from dependency:

$$\alpha_r = \frac{V_{y',r}}{V_{x',r}}, \tag{11}$$

$V_{x',c}, V_{y',c}$ are the components of the velocity of the mass center in the system $\{\}'$; they can be calculated as follows:

$$\alpha_f = -\delta + \frac{V_{y',f}}{V_{x',f}}. \tag{12}$$

$V_{x,c} = \dot{x}_c, V_{y,c} = \dot{y}_c$ are components of the velocity of the vehicle's mass center in the inertial system $\{\}$.

Table 1

Methods for determining the forces of road impact on vehicle

Value	Variant 1 (V1)	Variant 2 (V2)	Variant 3 (V3)
Longitudinal force	$f_{x',r} = f_{x'f} = \frac{1}{2}F_w + k(V_{nom} - V_{x',c})$, k – constant		
Lateral force	$f_{y',r} = -\alpha_r * F_{z,r}$ $f_{y',f} = -\alpha_f * F_{z,f}$	$f_{y',r} = -2C_r \tan\alpha_r$ $f_{y',f} = -2C_f \tan\alpha_f$	$f_{y',r} = -k_r\alpha_r F_{z,r}$ $f_{y',f} = -k_f\alpha_f F_{z,f}$ k_r, k_f – constants
Stabilizing moments	$M_{z',r} = M_{z',f} = 0$		$M_{z',p} = -f_{y',p} * a_1$ $-f_{x',p} * a_2 \tan\alpha_p$ where: $p \in \{r, f\}$, a_1, a_2 – constants

Method 3 was introduced so that the stabilizing forces and moments were determined in the same way as in the Dugoff-Uffelman model used in the spatial model. $F_{z,r}, F_{z,f}$ are forces normal to the plane x, y, determined from the following formulas:

$$F_{z,r} = \frac{m\bar{g}lf}{lr + lf}, \tag{13}$$

$$F_{z,f} = \frac{m\bar{g}lr}{lr + lf}, \tag{14}$$

where: $\bar{g} = g\cos\alpha$,
g – acceleration of gravity,
α – angle of the road to the x-axis.

The correctness of this vehicle model was evaluated. First of all, the simulation results obtained in our own program were compared with the experimental results. Then, the task of dynamic optimization for two vehicle motion maneuvers (lane change, overtaking) was formulated. The results obtained in the optimization process were applied to the vehicle control in the full model. The obtained runs of selected parameters characterizing the vehicle motion were compared.

4. MODEL VALIDATION

As part of this study, the proposed model with three degrees of freedom was validated. It consisted in comparing the results of the modeling of the passenger vehicle motion's dynamics with the experimental results reported in the literature [5]. In this study, selected vehicle motion parameters were recorded on a curved track with variable speed. In order to correctly map the vehicle motion trajectory, in the simulation calculation, the longitudinal speed of the vehicle $V_{x',c}$ was considered in the direction of the front wheel steering angles δ registered in the investigation (Figs. 4a and b). The speed of the vehicle during the experiment did not exceed 25 km/h. The parameters adopted in the simulation model are shown in Table 2.

Fig. 5 shows a comparison of the vehicle motion trajectory in the plane xy for data from the simulation model and experiment (E) (black dashed line). The implications of many ways of determining the forces of roadway impact on the vehicle were studied. Similar and acceptable compliance of vehicle motion trajectory mapping was obtained for methods V2 and V3. The maximum and minimum vehicle displacements in both cases did not differ by more than 2 m from those recorded in the experiment. In contrast, insufficient modeling accuracy was obtained for method V1. The vehicle displacements in the direction of the x and y axes with the inclusion in the model of all the considered ways of modeling the forces of roadway impact on wheels are presented in Fig. 6. In the absence of vehicle data, no results are reported for the SM (10 DoF).

Table 2

Passenger car details adopted for validation

Parameter	Symbol	Value	Unit
Distance of the front wheel axle from the center of gravity	l_f	1.25	m
Distance of the rear wheel axle from the center of gravity	l_r	1.32	m
Mass moment of inertia of the vehicle	$I_{z'}$	3411.52	kg·m^2
Vehicle mass	m	2160	kg

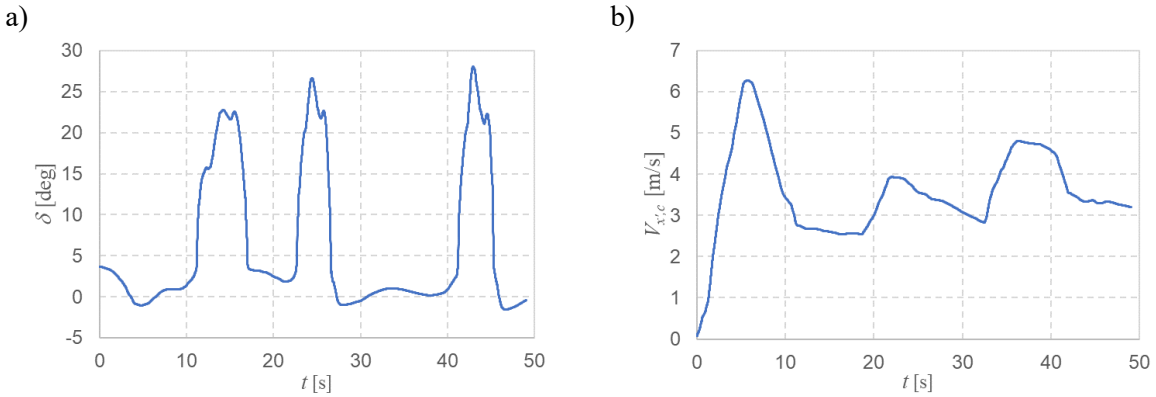

Fig. 4. (a) Front wheel steering angle δ and (b) the longitudinal velocity of the passenger car $V_{x',c}$ according to the literature [5]

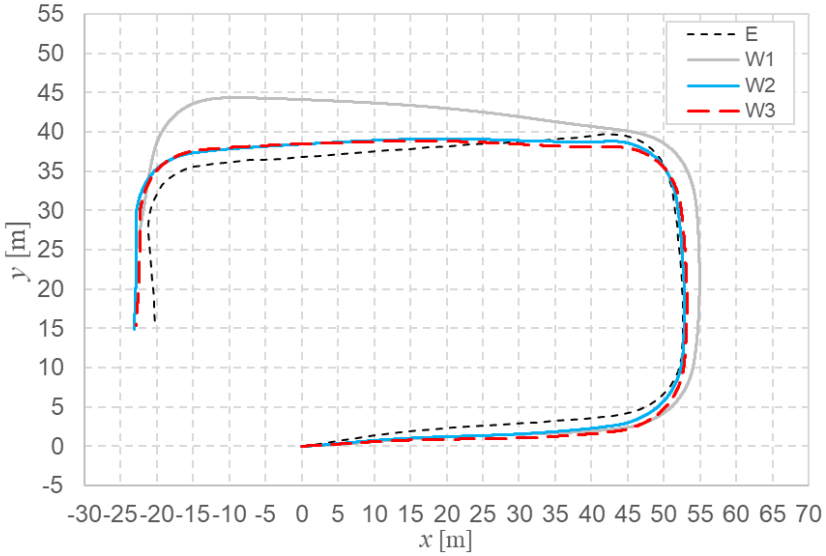

Fig. 5. Vehicle motion trajectory for all considered roadway-to-wheel impact modeling options

A motion simulation of a vehicle with the parameters shown in Table 3 was performed in order to evaluate the performance of the two models presented above.

Trajectories of the motion of a vehicle driving at 10, 14, and 18 m/s and of the front wheel steering angle forces were compared (Fig. 7).

a) b)

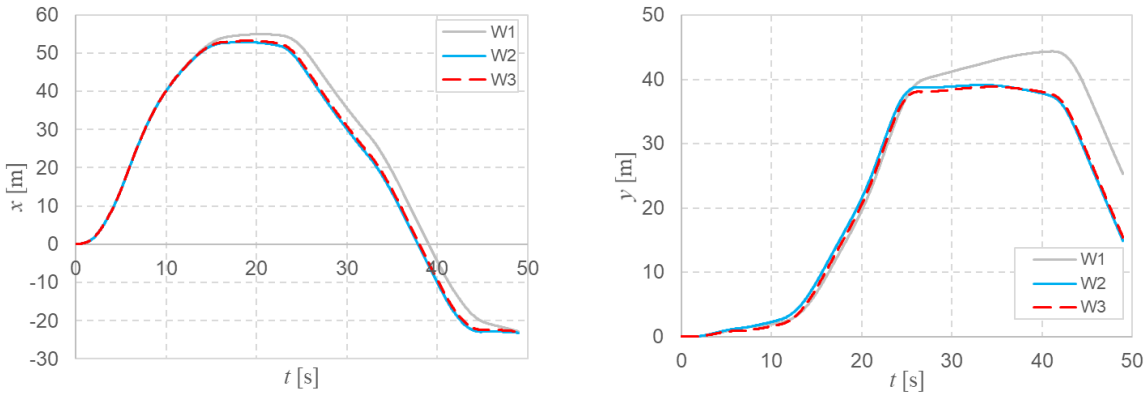

Fig. 6. Vehicle displacement in the direction of the (a) x-axis and (b) y-axis

Table 3

Passenger car details

Parameter	Symbol	Value	Unit
Distance of the front wheel axle from the center of gravity	l_f	1.2	m
Distance of the rear wheel axle from the center of gravity	l_r	1.2	m
Distance between front and rear wheels	b_f, b_r	1.2	m
Mass moment of inertia of the vehicle acting relative to the z'-axis	$I_{z'}$	300	kg·m^2
Mass moment of inertia of the vehicle acting relative to the x'-axis	$I_{x'}$	100	kg·m^2
Mass moment of inertia of the vehicle acting relative to the y'-axis	$I_{y'}$	250	kg·m^2
Vehicle mass	m	600	kg
Wheel radius	r_w	0.3	m
Mass moment of inertia of a wheel	I_w	0.54	kg·m^2
Wheel mass	m_w	20	kg

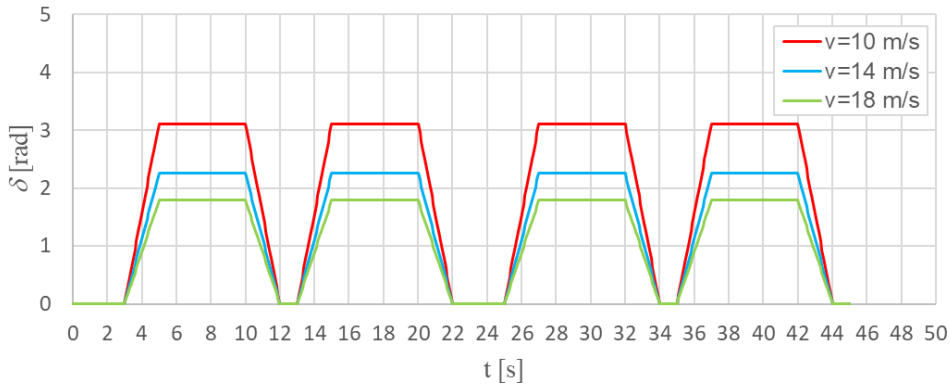

Fig. 7. Adopted front wheels steering angle δ

The trajectories obtained for the SM and BM (BM with the V3 variant) are shown in Fig. 8.

Table 4 compares simulation calculation times $\bar{t}_c$ for both models in the range of $t \in \langle 0; 45 \rangle$ s for a constant integer step $h = 0.01$ s. The calculations were performed on a personal computer with an Intel Xenon Gold 5220 CPU 2.2 GHz and 64 GB of RAM. This time is two orders of magnitude smaller in the BM than in the SM. This suggests that the simplified model should be used to solve the dynamic

optimization problem when the vehicle motion equations must be repeatedly integrated over the entire simulation time to find the optimal value.

The vehicle motion trajectories in the initial phase (forward, first turn) are similar in all cases analyzed. However, with an increase in vehicle speed, differences in displacement between models begin to be noticeable. In the final motion phase, when the vehicle displacement in the direction of the x-axis is close to 0 m, if the vehicle travels at 10 m/s, the difference of displacements in the direction of the y-axis between the two models with respect to the width of the trajectory w_y per the BM is only 0.17%. However, at a speed of 18 m/s, this difference increases to 1.28%.

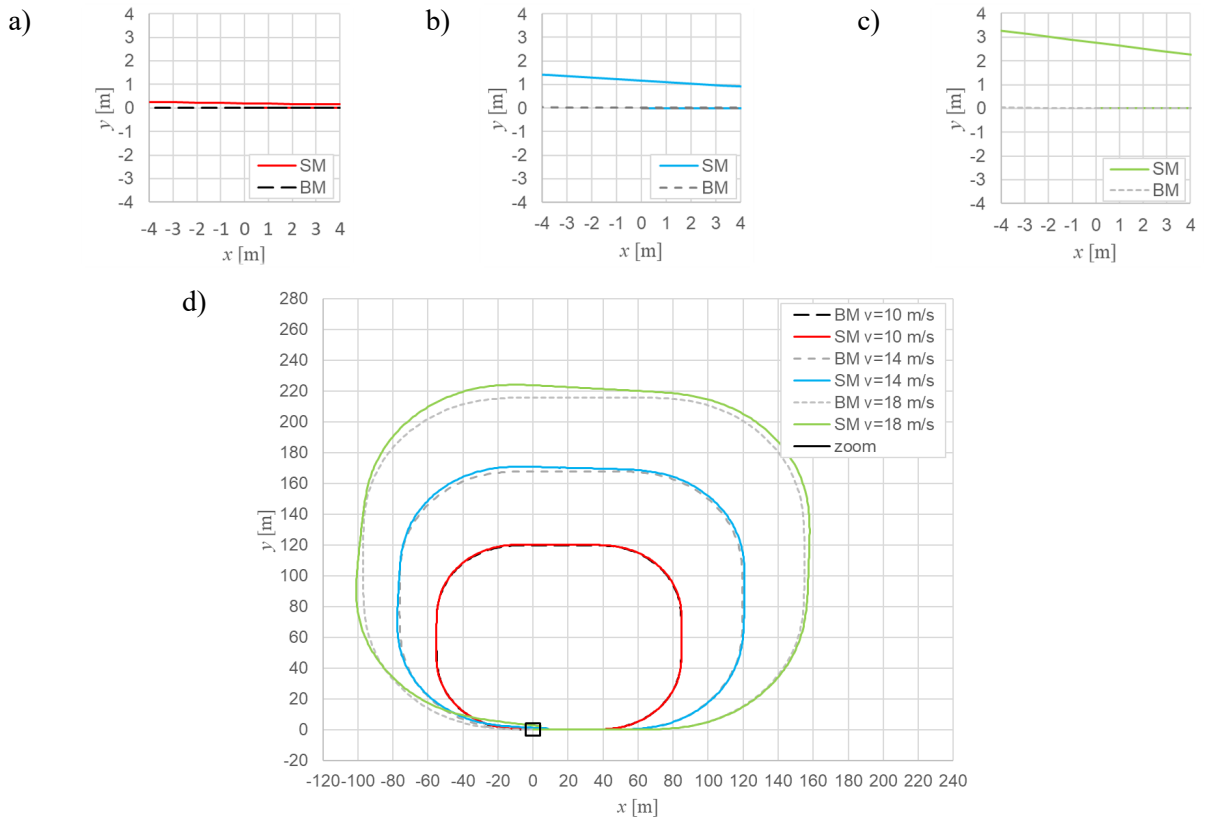

Fig. 8. Vehicle motion trajectory according to the BM and SM for different vehicle speeds v: a) zoom for v=10 m/s, b) zoom for v = 14 m/s, c) zoom for v = 18 m/s, d) all considered vehicle speeds

Table 4

Simulation calculation times and vehicle motion trajectory parameters

Nominal velocity of vehicle v_{nom} [m/s]	Width of vehicle trajectory (BM)		Horizontal position of the vehicle y [m] when $x = 0$ m and $t > 40$ s		Calculation time $\bar{t}_c$ [s]	
	in the x-axis direction w_x [m]	in the y-axis direction w_y [m]	BM	SM	BM	SM
10	139.838	119.838	0	0.204	0.03	2.73
14	195.850	167.866	0.022	1.168		
18	251.853	215.86	0.015	2.771		

The validated vehicle motion model (BM) was then applied to solve the dynamic optimization task. This entailed finding the appropriate front wheel steering angles at selected points in time, ensuring the implementation of lane change and overtaking maneuvers. The results of numerical simulations presented further in this paper were obtained using the third roadway impact modeling option (V3).

5. DYNAMIC OPTIMIZATION

When developing a reliable autonomous vehicle control algorithm, a number of factors are taken into consideration. The number of such factors should be as small as possible and ensure that an acceptable solution is found in the shortest possible time. The procedure presented in this part of the study used the simplified vehicle model presented earlier, which made it possible to accurately map the lane change maneuver (task T1) and the overtaking maneuver (task T2) in close to real time. The correct implementation of both maneuvers required the formulation of two separate dynamic optimization tasks. In both cases, the front wheel steering angles δ were selected for a specific time t. It was assumed that the front wheel steering angles for both maneuvers in the BM were as shown in Fig. 9.

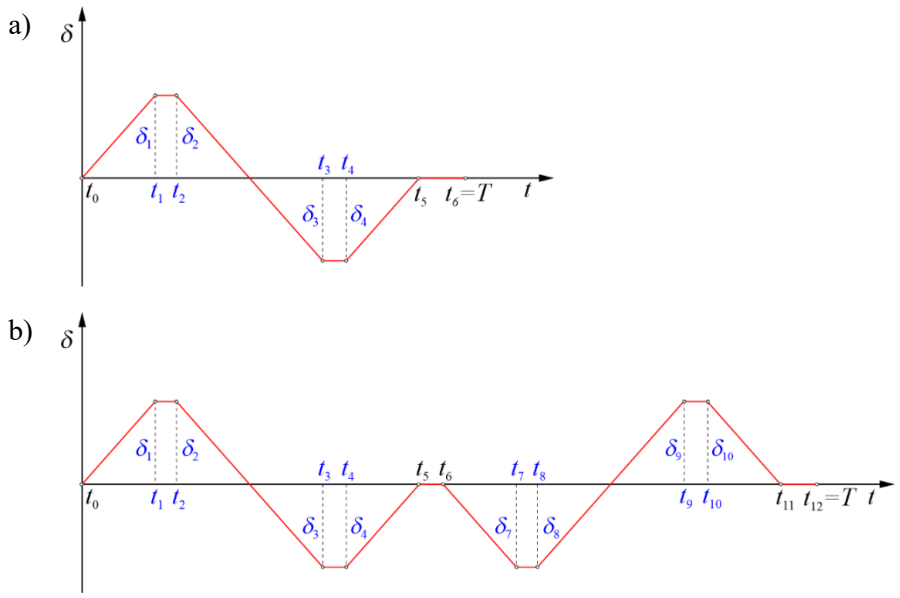

Fig. 9. Front wheel steering angles δ for the a) lane change maneuver - task T1 and b) overtaking maneuver – task T2

In Task T1, four front wheel steering angles are observed for δ_i at points $t_1 \div t_4$. Between $t_{i-1}\ a\ t_i$, the angle δ changes linearly from δ_{i-1} to δ_i. $\delta(t_0) = \delta(t_5) = \delta(t_6 = T) = 0$ was then assumed. In contrast, task T2 looked for eight values $\delta(t_i)$ for $i = 1, 2, 3, 4$ and $\delta(t_{i+2})$ for $i = 5, 6, 7, 8$, assuming $\delta(t_0) = \delta(t_5) = \delta(t_6) = \delta(t_{11}) = \delta(t_{12} = T) = 0$.

After a preliminary analysis of the simulation results, the number of decision variables n may be reduced. Therefore,

<u>in Task T1:</u>
$n = 1$; when it is assumed $\delta(t_1) = \delta(t_2) = X_1, \delta(t_3) = \delta(t_4) = -X_1$,
$n = 2$; $\delta(t_1) = \delta(t_2) = X_1, \delta(t_3) = \delta(t_4) = X_2$,
$n = 4$; $\delta(t_1) = X_1, \delta(t_2) = X_2, \delta(t_3) = X_3, \delta(t_4) = X_4$,

<u>in Task T2:</u>
$n = 1$; $\delta(t_1) = \delta(t_2) = X_1, \delta(t_3) = \delta(t_4) = -X_1$,
$\delta(t_7) = \delta(t_8) = -X_1$, $\delta(t_9) = \delta(t_{10}) = X_1$,
$n = 2$; $\delta(t_1) = \delta(t_2) = X_1$, $\delta(t_3) = \delta(t_4) = X_2$,
$\delta(t_7) = \delta(t_8) = X$, $\delta(t_9) = \delta(t_{10}) = X_1$,
$n = 4$; $\delta(t_1) = X_1$, $\delta(t_2) = X_2$, $\delta(t_3) = X_3$, $\delta_4 = X_4$,
$\delta(t_7) = X_4$, $\delta(t_8) = X_3$, $\delta(t_9) = X_2, \delta(t_{10}) = X_1$.

The task of dynamic optimization is to search for such a function value that the minimum is achieved by the following function:

$$\delta = \delta(X_1, X_2, \dots, X_n) \tag{15}$$

Task T1 - lane change:

$$\Omega = \Omega(X_1, X_2, \dots, X_n) = \left[\frac{1}{(T - t_5)} \int_{t_5}^{T} (y - d)^2 \, dt\right]^{\frac{1}{2}} + \left[\frac{1}{(T - t_5)} \int_{t_5}^{T} \psi^2 \, dt\right]^{\frac{1}{2}}, \tag{16}$$

Task T2 – overtaking:

$$\begin{aligned} \Omega = \Omega(X_1, X_2, \dots, X_n) = &\left[\frac{1}{(t_6 - t_5)} \int_{t_5}^{t_6} (y - d)^2 \, dt\right]^{\frac{1}{2}} + \left[\frac{1}{(t_6 - t_5)} \int_{t_6}^{t_5} \psi^2 \, dt\right]^{\frac{1}{2}} \\ &+ \left[\frac{1}{(T - t_{12})} \int_{t_{12}}^{T} y^2 \, dt\right]^{\frac{1}{2}} + \left[\frac{1}{(T - t_{12})} \int_{t_{12}}^{T} \psi^2 \, dt\right]^{\frac{1}{2}}. \end{aligned} \tag{17}$$

where: y – displacement of the vehicle's mass center in the direction of the y-axis of the inertial system {},

ψ – angle of inclination of the vehicle's longitudinal axis to the x inertial system {} axis

d – distance between the adjacent lane axes,

X_i – decision variables.

subject to the following constraints:

$$X_i^{min} \le X_i \le X_i^{max} \; i = 1, \dots, n \tag{18}$$

where: X_i^{min}, X_i^{max} – minimum and maximum permissible front wheel steering angles δ.

The optimization task was solved for various numbers of decision variables X_i. The optimization task was solved for the vehicle parameters listed in Table 3. The Nelder-Mead simplex method was used for optimization [7]. At each optimization step, it was necessary to integrate the motion equations in the interval $\langle 0; T \rangle$ to enable the functional value calculation Ω from (12).

In the first task (T1), on changing the lane, it was assumed that the maneuver was performed in time T = 20 s, and the front wheel steering function values were searched for at the following times: t_1 = 3 s, t_2 = 4 s, t_3 = 10 s, and t_4 = 11 s. The distance between adjacent lanes d was adopted at 3.5 m. The same distance between the adjacent lane axes was also assumed in Task T2. The total simulation time for the overtaking maneuver in Task T2 was extended to T = 35 s. Function values δ were observed at eight points on the timeline $t \in [3, 4, 10, 11, 18, 19, 25, 26]$ s. In both tasks, it was assumed that the vehicle during the simulation moves at a constant speed. A solution to the optimization problem for various motion speeds was sought.

The course of function δ in Task T1 for various vehicle motion speeds obtained after the assumption n = 1 is shown in Fig. 10a. As can be seen, the higher vehicle motion speed forced the choice of smaller steering angles. The vehicle mass center's displacement in the direction of the y-axis (Fig. 11a), starting from 14 s of simulation, is close to the assumed distance d = 3.5 m. Also, the angle of inclination of ψ the vehicle's longitudinal axis to the x-axis in the final phase of the maneuver was close to zero (Fig. 11b). This means that after the lane change maneuver, the vehicle can continue straight ahead (along the lane axis).

The optimization results obtained after solving Task T2 are shown in Figs. 10b and 12. The front wheel steering angles δ were selected for various numbers of decision variables n and the vehicle speed V_{nom} = 20 m/s. The solutions obtained for $n = 1$ and $n = 2$ are almost identical, whereas the solution obtained for four decision variables differed slightly from the two previous solutions. The difference is due to the fact that at different moments in time (t_1 and t_2, t_3 and t_4, t_7 and t_8 and t_9 and t_{10}) different values of δ could be found. As was the case with the first task, all results obtained in the second task were also of acceptable accuracy. In the time interval $t\epsilon \langle 14; 15 \rangle$ s, the vehicle's lateral displacement

was approx. 3.5 m, and the angle ψ was close to 0. At the end of the overtaking maneuver, the displacement y and the angle ψ were close to zero.

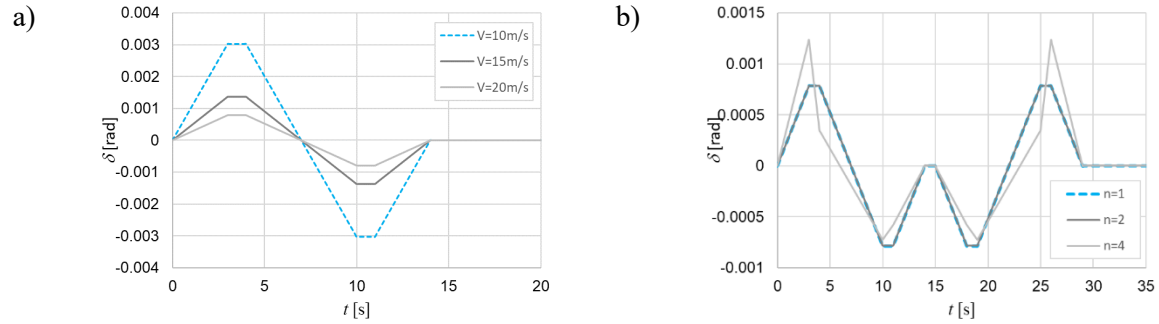

Fig. 10. Curves of front wheel steering angle δ: a) Task T1 and b) Task T2

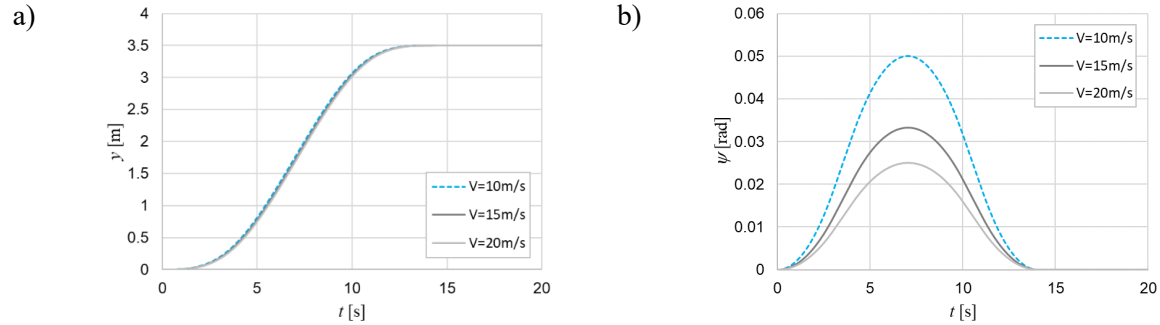

Fig. 11. a) Vehicle displacement in the direction of the y-axis and b) the angle of inclination ψ of the vehicle's longitudinal axis to the x-axis (Task T1)

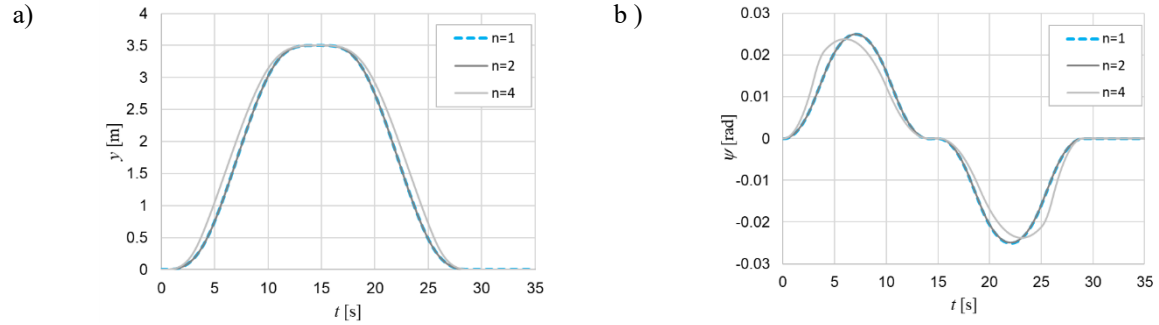

Fig. 12. a) Vehicle displacement in the direction of the y-axis and b) inclination angle ψ of the vehicle's longitudinal axis to the x-axis – Task T2

The results presented in Table 5 show that the time needed to find a final solution with the applied optimization method depends, inter alia, on vehicle speed V_{nom} and the number of decision variables n. Increasing the number of decision variables from one to four results in four times the number of iterations performed and, thus, a four-times longer calculation time. Moreover, a lower vehicle motion speed translates into more optimization steps. The calculation times were recorded by integrating the motion equations with a constant step $h = 0.01$ s.

The correctness of the solutions obtained in optimization was verified. The functions δ obtained in the simplified model (3 DoF) were used as inputs in the full model (10 DoF). The vehicle motion dynamics results obtained in both models are compared in Figs. 13 and 14. The courses of lateral displacement of the vehicle y and the angle of the vehicle body ψ were compared. Additional plots showing the differences between the compared values Δy and $\Delta\psi$ were created to better illustrate the differences between the two models.

Table 5

Time required to solve the optimization problem

Maneuver	Vehicle speed V_{nom} [m/s]	Number of decision variables n	Number of optimization steps N	Time of calculation [s]
Lane change (T1)	10	1	39	0.24
	15	1	29	0.21
	20	1	33	0.19
Overtaking (T2)	20	1	33	0.33
	20	2	70	0.69
	20	4	136	1.22

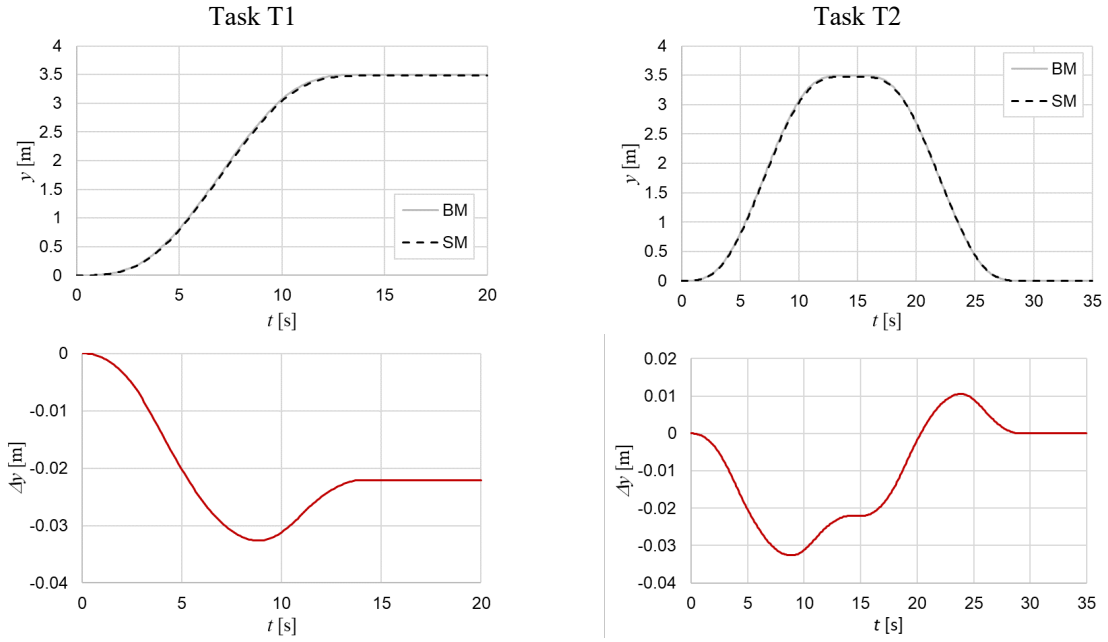

Fig. 13. Vehicle displacement in the direction of the y-axis and the displacement differences between them Δy – Tasks T1 and T2

The simulation results were obtained assuming that the vehicle was moving at the speed of V_{nom} = 10 m/s. The largest difference in lateral displacement Δy between the two models of more than 0.03 m was obtained at the initial phase of the simulation. In the T1 task, the difference Δy at the end of the simulation was -0.02 m. This means that the vehicle in the BM had a smaller lateral displacement. In the case of the overtaking maneuver, the difference Δy at time t = 20 s was zero. Furthermore, the difference $\Delta\psi$ = 0 in both models was obtained at the beginning and end of the simulation. Its largest value was recorded at 5 s of the simulation, and it was less than 1% of the angle ψ value. The maximum displacement Δy and maximum angle $\Delta\psi$ differences did not exceed ±0.04 m and ±0.004 rad, respectively. This outcome indicates good agreement between the two compared vehicle dynamics models. The smaller number of generalized coordinates in the BM needed to describe the vehicle dynamics significantly reduced the calculation time. The calculation time for solving the dynamic optimization problem using the simplified 3 DoF model was almost 150 times shorter than for the full 10 DoF model.

6. CONCLUSIONS

Controlling an autonomous vehicle requires the vehicle's behavior to be predicted over time, considering current external factors. The parameters with fundamental impacts on the vehicle motion

trajectory include the vehicle speed and the front wheel steering angles. This paper presented two simplified models of the vehicle: a spatial SM with 10 degrees of freedom and a flat model with three degrees of freedom. The validation of the models indicates that it is possible to correctly reflect the movement of the real vehicle. As a part of the validation of the BM, the course of speed and steering angle were assumed as in the experiment [5]. The trajectories of the vehicle obtained in the simulation differed slightly from the trajectory in the experiment. The SM was validated indirectly by comparing the results of calculations according to this model with the results of the BM. A similar method of determining road forces acting on the wheels was used in both models, and the results were virtually the same.

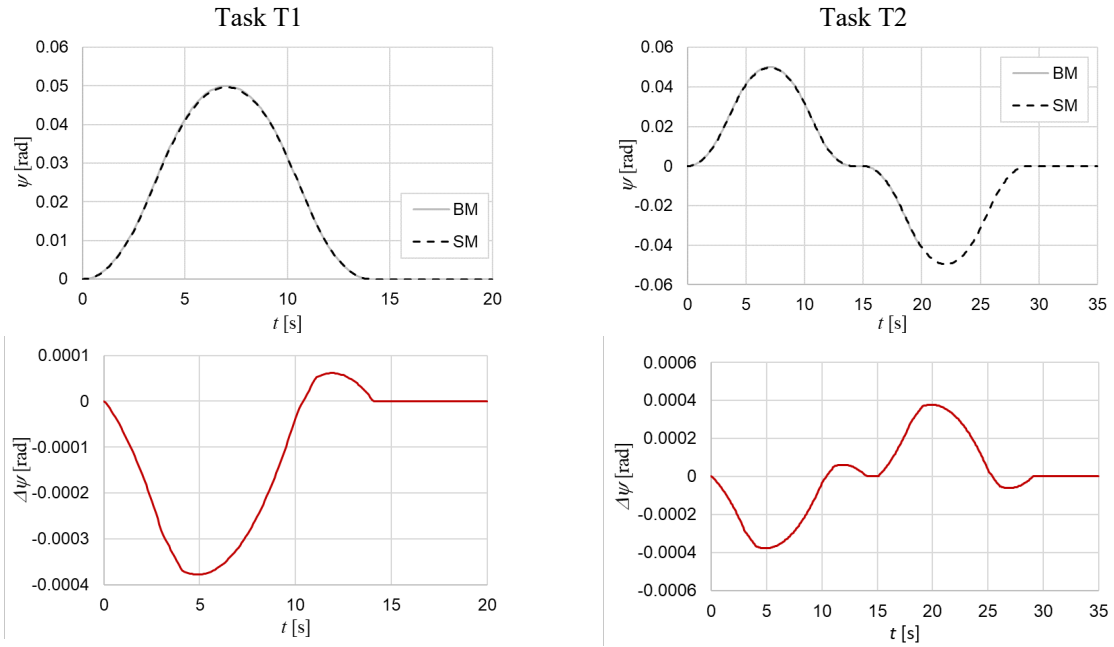

Fig. 14. Inclination angle ψ of the vehicle's longitudinal axis to the x-axis and the inclination angle differences between them $\Delta\psi$ – Tasks T1 and T2

The BM was used to determine the courses of the steering angle (function δ(t)) in lane changing and overtaking maneuvers. Appropriate optimization tasks were formulated for this purpose, which were solved using the downhill simplex method. An important feature of these tasks is the need to integrate the equations of vehicle motion in each optimization step (for each combination of decision variables). The solution of the dynamic optimization task in the BM for a lane change or overtaking maneuver takes less than 0.3 s. The courses of δ(t) obtained as a result of optimization using the BM were applied to the SM, and a very good level of compliance was achieved between the courses of parameters describing vehicle motion. It is noteworthy that the adoption of steering angle values at discrete moments of time as decision variables and the use of linear interpolation between points t_i enabled a reduction in the number of these variables. The developed computer program allowed the use of more complex forms of the δ(t) function (e.g., exponential or splain functions).

When the objective function is formulated, it is insufficient to provide the expected horizontal displacement of the vehicle due to lane changing. This makes it necessary to add a limitation factor for the deviation of the vehicle's longitudinal axis angle to the x-axis of the inertial system {} after the maneuver is completed. The proposed approach for reducing the number of decision variables significantly affects the number of optimization steps required. The simulation results obtained for optimization with a single decision variable in the lane change maneuver confirm correct vehicle trajectories.

The authors are hopeful that the presented models will have valuable practical applications because, for a finite set of vehicle motion parameters and road infrastructure geometry, it is possible to find a generalization of the model using artificial neural networks that provide vehicle control in close to real time. Work is also currently underway to increase the numerical efficiency of the SM, which, while

requiring more vehicle data, makes it possible to simultaneously account for vehicle tilts along the longitudinal and transverse axes. Thus, it will be possible to take into account cases of vehicle wheels lift-off from a road surface.

References

1. Adamiec-Wójcik, I. & Drąg, Ł. & Grzegożek, W. & Wojciech, S. Calibration of an articulated vehicle model and analysis of friction model in the connection between two vehicle units. *Journal of Computational and Nonlinear Dynamics*. 2019. Vol. 14(5). No. 051008. P. 1-12.
2. Brown, M. & Funke, J. & Erlien, S. & Gerdes, J.C. Safe driving envelopes for path tracking in autonomous vehicles. *Control Engineering Practice*. 2017. Vol. 61. P. 307-316.
3. Craig, J.J. *Introduction to Robotics: Mechanics a Control. Third edition*. Pearson Prentice Hall Person Education. Upper Saddle River. 2005. 408 p.
4. Grzegożek, W. & Adamiec-Wójcik, I. & Wojciech, S. *Komputerowe modelowanie dynamiki pojazdów samochodowych*. Wydawnictwo Politechniki Krakowskiej. Kraków 2003. 196 p. [In Polish: Grzegożek, W. & Adamiec-Wójcik, I. & Wojciech, S. *Computer modelling of vehicles.* Cracow University of Technology Press].
5. Guo, H. & Cao, D. & Chen, H. & Sun, Z. & Hu, Y. Model predictive path following control for autonomous cars considering a measurable disturbance: Implementation, testing, and verification. *Mechanical Systems and Signal Processing*. 2019. Vol. 118. P. 41-60.
6. Hu, C. & Qin, Y. & Cao, H. & Song, X. & Jiang, K. & Rath, J.J. & Wei, C. Lane keeping of autonomous vehicles based on differential steering with adaptive multivariable super twisting control. *Mechanical Systems and Signal Processing*. 2019. Vol. 125. P. 330-346.
7. Nelder, J.A. & Mead, R. Simplex method for function minimalization. *Computer Journal*. 1965. Vol. 7. P. 308-313.
8. Polański, A. *Komputerowy model do symulacji ruchu i zderzeń pojazdów wieloczłonowych, z uwzględnieniem tarcia w połączeniach między członami*. PhD thesis. ATH w Bielsku-Białej. 2005. 149 p. [In Polish: Polański A. *Computer model for the simulation of motion and collision of articulated vehicles, taking into account friction in the joints between links*. University of Bielsko-Biala].
9. Prochowski, L. & Ziubiński, M. & Szwajkowski, P. & Gidlewski, M. & Pusty, T. & Stańczyk, T.L. Impact of control system model parameters on the obstacle avoidance by an autonomous car-trailer unit: research results. *Energies*. 2021. Vol. 14. No. 10. P. 1-31.
10. Wnęk, H. *Analiza wpływu promienia zataczania na przebieg procesu hamowania pojazdu wyposażonego w ABS*. PhD thesis. ATH w Bielsku-Białej. 2005. 129 p. [In Polish: Wnęk H. *Analysis of offset radius on breaking process of vehicle equipped with ABS*. University of Bielsko-Biala].
11. Szczotka, M. & Wojciech, S. Application of joint coordinates and homogenous transformations of modeling vehicle dynamics. *Nonlinear Dynamics*. 2008. Vol. 52. P. 377-393.
12. Zhang, F. & Gonzales, J. & Li, S.E. & Borelli, F. & Li, K. Drift control for cornering maneuver of autonomous vehicles. *Mechatronics*. 2018. Vol. 54. P. 167-174.

Received 06.02.2022; accepted in revised form 05.06.2023